BIOPHARMACEUTICS & DRUG DISPOSITION
Biopharm. Drug Dispos. **33**: 378–402 (2012)
Published online 4 September 2012 in Wiley Online Library
(wileyonlinelibrary.com) **DOI**: 10.1002/bdd.1803

Mechanistic analysis of solute transport in an *in vitro* physiological two-phase dissolution apparatus

Deanna M. Mudie[a], Yi Shi[b], Haili Ping[a,†], Ping Gao[b], Gordon L. Amidon[a], and Gregory E. Amidon[a,*]
[a]*University of Michigan, College of Pharmacy, Ann Arbor, MI, USA*
[b]*Abbott Laboratories, North Chicago, IL, USA*

ABSTRACT: *In vitro* dissolution methodologies that adequately capture the oral bioperformance of solid dosage forms are critical tools needed to aid formulation development. Such methodologies must encompass important physiological parameters and be designed with drug properties in mind. Two-phase dissolution apparatuses, which contain an aqueous phase in which the drug dissolves (representing the dissolution/solubility component) and an organic phase into which the drug partitions (representing the absorption component), have the potential to provide meaningful predictions of *in vivo* oral bioperformance for some BCS II, and possibly some BCS IV drug products. Before such an apparatus can be evaluated properly, it is important to understand the kinetics of drug substance partitioning from the aqueous to the organic medium. A mass transport analysis was performed of the kinetics of partitioning of drug substance solutions from the aqueous to the organic phase of a two-phase dissolution apparatus. Major assumptions include pseudo-steady-state conditions, a dilute aqueous solution and diffusion-controlled transport. Input parameters can be measured or estimated *a priori*. This paper presents the theory and derivation of our analysis, compares it with a recent kinetic approach, and demonstrates its effectiveness in predicting *in vitro* partitioning profiles of three BCS II weak acids in four different *in vitro* two-phase dissolution apparatuses. Very importantly, the paper discusses how a two-phase apparatus can be scaled to reflect *in vivo* absorption kinetics and for which drug substances the two-phase dissolution systems may be appropriate tools for measuring oral bioperformance. Copyright © 2012 John Wiley & Sons, Ltd.

Key words: dissolution; oral absorption; two-phase; biphasic; physiological

Introduction

Pharmaceutical solid oral dosage forms must dissolve in the gastrointestinal lumen and absorb into the intestinal membrane before reaching the systemic circulation. The rate and extent of drug dissolution and absorption depend on the characteristics of the active ingredient such as pK_a, crystal form and solubility, as well as properties of the dosage form [1]. Just as importantly, characteristics of the physiological environment such as buffer species, pH, bile salts, gastric emptying rate, intestinal liquid volume, intestinal motility and shear rates significantly impact dissolution and absorption [2]. While scientists have used *in vitro* test methods for many years, no single test or apparatus accurately captures the range of key *in vivo* conditions that have the potential to affect the relative rates and extents of *in vivo* dissolution and absorption for the range of diverse drug products. Due to the difficulty in

*Correspondence to: The University of Michigan, College of Pharmacy/Office 2062, 428 Church Street, Ann Arbor, MI 48109-1065, USA.
E-mail: geamidon@umich.edu
†Current address: Food and Drug Administration, Washington, DC.

Received 19 March 2012
Revised 1 June 2012
Accepted 18 July 2012

developing a 'one size fits all' physiological dissolution apparatus, it is helpful to use the physicochemical characteristics of the drug and dosage form to design a dissolution test that captures the key physiological conditions that have the potential to affect the oral bioperformance. For example, capturing the pH profile encountered when a drug travels from the acidic stomach to the less acidic small intestine is important for low-solubility weak acids and bases with pK_as in the physiological range, whereas the type and concentration of bile salts in the dissolution medium rather than the pH profile is important for low-solubility neutral compounds.

The Biopharmaceutics Classification System (BCS) attempts to categorize *in vivo* oral bioperformance based on a drug's solubility, extent of permeation and *in vitro* testing results [3]. It has had a significant effect on the regulatory environment as the Food and Drug Administration (FDA) and World Health Organization (WHO) consider biowaivers for some drugs [4]. The BCS classification of a drug can be used as a general guideline to predict whether solubility, dissolution rate, or permeation rate will be the rate-limiting step in reaching the systemic circulation. However, even drugs within a single BCS class have a range of solubilities, effective human intestinal permeation rates, particle sizes, doses and dosage forms, all of which may contribute to differences in dissolution and absorption characteristics *in vivo*. Therefore, for drugs that fall within BCS II, III or IV, using its BCS classification alone to design the appropriate dissolution test has some limitations. For instance, performing a USP dissolution test in a non-physiological volume of buffer (i.e. 900 ml) to predict *in vivo* performance for certain BCS Class II (low solubility, high permeation) drugs may lead to poor *in vitro–in vivo* correlations (IVIVCs) due to an unrealistic degree of drug saturation in the dissolution medium, leading to *in vitro* dissolution rates that do not reflect the *in vivo* situation.

Two-phase dissolution apparatuses can evaluate simultaneously the kinetics of both drug dissolution and partitioning, and can simulate drug absorption while using a physiological volume of aqueous fluid (~100 ml in fasted humans [5]). These systems contain a volume of aqueous medium in which the drug dissolves and a second volume of an immiscible organic medium (e.g. 1-octanol) that allows drug partitioning from the aqueous medium. If designed properly, the rate of appearance of drug in the organic phase is expected to be similar to the rate of absorption *in vivo*. Assuming that an appropriate interfacial surface-area-to-volume ratio between the aqueous and organic phases is used, the organic phase can help to maintain physiologically relevant saturation conditions in the aqueous phase and physiologically relevant partitioning kinetics for some potential drug candidates.

Researchers have been exploring the utility of two-phase systems for novel dosage forms such as lipid-filled capsules and controlled-release dosage forms, as well as immediate-release dosage forms since the 1960s. Pillay and Fassihi employed a two-phase method to study the dissolution of poorly-soluble nifedipine from a lipid-based capsule formulation [6]. Their purpose was to circumvent the possible precipitation of the drug as well as analytical difficulties associated with lipid-based capsule formulations. Hoa and Kinget, as well as Gabriels and Plaizier-Vercammen, developed two-phase methods to overcome difficulties in maintaining sink conditions for poorly soluble anti-malarial drugs such as arteminsinin, dihydroartemisinin and artemether, that occurred using single-phase dissolution methods [7,8]. Grundy *et al*. developed a two-phase system to measure release from the nifedipine gastrointestinal therapeutic system (GITS), a push–pull osmotic system, to maintain sink conditions and to develop an *in vitro–in vivo* correlation that could not be achieved with other dissolution methods such as the flow-through and differential (ALZA) method [9]. More recently, Heigoldt *et al*. performed dissolution testing of modified release formulations of two weakly basic BCS II drugs in a two-phase ('biphasic') dissolution test with a pH gradient in the aqueous medium [10]. They found the test to be 'qualitatively predictive' of the *in vivo* performance and found it to be superior to single-phase dissolution testing at a single pH. Shi *et al*. used a two-phase dissolution apparatus that incorporated both a USP II vessel and a USP IV flow-through cell successfully to differentiate between three formulations of celeboxib and to generate a rank-order relationship between the amount of drug in the organic phase at 2 h and the *in vivo* area under the

DOI: 10.1002/bdd

plasma concentration–time curve (*AUC*) or maximum plasma concentration (C_{max}) [11].

While two-phase systems have shown improvement over conventional methods in some cases, limited work has been undertaken to elucidate the mechanism by which they may facilitate improved IVIVCs over single phase systems and determine for which types of drugs and drug products they could be most useful. The purpose of this work is to perform a mass transport analysis of the kinetics of partitioning of drugs in solution from the aqueous to the organic phase of a two-phase dissolution apparatus. While other researchers have provided mathematical analyses, we use a mechanistic approach to understand the drug transport phenomenon within the system [12,13]. This paper presents the theory and derivation of our model and compares it with an existing kinetic model. It demonstrates the effectiveness of our analysis in predicting experimental results in four different *in vitro* two-phase dissolution apparatuses using the BCS II weak acids ibuprofen, nimesulide and piroxicam. More importantly, this paper outlines how a two-phase dissolution apparatus can be scaled to be physiologically relevant and to reflect *in vivo* absorption kinetics and to discuss for which types of drug substances a two-phase system may be most useful.

Material and Methods

Nomenclature

A_I	Surface area of the aqueous–organic interface
C_a	Total concentration on ionized and non-ionized drug in the bulk aqueous phase
$C_{a,t}$	Total, time-dependent concentration on ionized and non-ionized drug in the bulk aqueous phase
C_o	Concentration of drug in the bulk organic phase
$C_{o,t}$	Time-dependent concentration of drug in the bulk organic phase
C_o'	Concentration of drug in the bulk organic phase, corrected for partition coefficient
D_a	Diffusion coefficient in the aqueous phase
D_o	Diffusion coefficient in the organic phase
h_a	Aqueous diffusion layer thickness
F_a	Fraction absorbed into the intestinal membrane *in vivo*
F_o	Fraction of solute in the organic medium
$F_{o,\infty}$	Fraction of solute in the organic medium at equilibrium
$H_{a,i}$	Concentration of hydrogen ions on the aqueous side of the interface
h_o	Organic diffusion layer thickness
j	Pseudo-steady-state flux of drug across the aqueous and organic diffusion layers
j_a	Pseudo-steady-state flux across the aqueous diffusion layer
j_o	Pseudo-steady-state flux across the organic diffusion layer
k_a	First-order absorption rate constant from pharmacokinetics
k_{aq}	Mass transfer coefficient across the aqueous diffusion layer
k_{org}	Mass transfer coefficient across the organic diffusion layer
K	Drug partition coefficient in the aqueous and organic media (non-ionized species)
K_a	Equilibrium constant of the drug association reaction in the aqueous medium
K_{ap}	Drug apparent partition coefficient in the aqueous and organic media at the interfacial pH
$K_{ap,t}$	Time-dependent apparent partition coefficient of drug in the aqueous and organic media at the interfacial pH
M_T	Total mass of dissolved drug in the system
P_I	Drug interfacial permeation rate across the aqueous and organic diffusion layers
$R_{a,b}$	Concentration of ionized species in the bulk aqueous phase
$R_{a,i}$	Concentration of ionized species on the aqueous side of the interface
$RH_{a,b}$	Concentration of non-ionized species in the bulk aqueous phase
$RH_{a,i}$	Concentration of non-ionized species on the aqueous side of the interface
$RH_{o,b}$	Concentration of non-ionized species in the bulk organic phase
$RH_{o,i}$	Concentration of non-ionized species on the organic side of the interface
t	Time
t_{res}	Residence time in the small intestine
V_a	Total volume of aqueous medium
V_o	Total volume of organic medium
β	Equal to $V_a/(K_{ap}*V_o)$

DOI: 10.1002/bdd

Description of the apparatus

Figure 1 is a schematic of a two-phase dissolution apparatus. It consists of a flat- or round-bottom glass vessel that is maintained at constant temperature. It contains both aqueous and organic media that are present in two distinct layers, and are agitated by a single shaft fitted with two impellers. At the beginning of the experiment, dissolved drug is added directly to the aqueous medium. Partitioning of the drug from the aqueous to the organic medium is monitored as a function of time until the equilibrium concentration of drug in each phase is reached.

Derivation of the model

The kinetics of partitioning of drug from the aqueous to the organic phase of a two-phase system is described based on a physical model approach Suzuki *et al*. originally developed to describe simultaneous chemical equilibria and mass transfer of basic and acidic solutes through lipoidal barriers [14]. It is assumed that drug transport is controlled by diffusional resistance arising from a hydrodynamically controlled or 'stagnant' diffusion layer on each side of the aqueous–organic interface, and the steady diffusion across a thin film approximation is used to predict the total flux of drug across the two diffusion layers in series. Model assumptions are as follows.

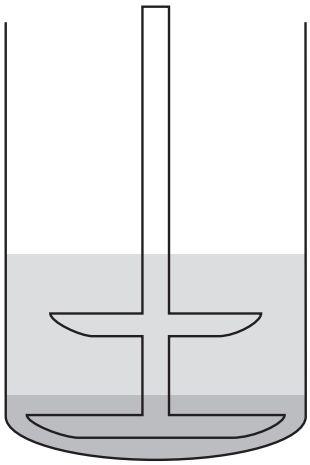

Figure 1. Schematic diagram of a two-phase dissolution apparatus

1. The diffusion coefficient in each medium is not concentration dependent and aqueous diffusion coefficients of ionized and non-ionized drug are equal.
2. Aqueous and organic media behave as ideal solutions.
3. Drug transport via convection is minimal and can be neglected.
4. An initial bolus of drug in solution is injected into the aqueous medium and the net flux of drug occurs in one direction across each diffusion layer from the well-mixed, bulk aqueous medium to the well-mixed, bulk organic medium.
5. The instantaneous concentration profile within each diffusion layer resembles a steady state (pseudo-steady-state approximation).
6. Drug concentrations at the aqueous and organic sides of the interface are in equilibrium.
7. Drug transfer across the aqueous–organic interface is instantaneous.
8. Mass transfer from the aqueous to the organic medium occurs only through the interface.
9. Concentration of dissolved drug in either phase is not affected by processes such as chemical reaction, degradation, precipitation, etc.
10. The thickness of each diffusion layer is constant with time.

Figure 2 is a schematic diagram of a two-phase system tipped on its side, to which a monoprotic weak acid has been added to the aqueous buffer. The first transport step is the diffusion of ionized and non-ionized drug across the aqueous diffusion layer of thickness h_a. According to Fick's First Law and using assumptions 1–5, the flux across the

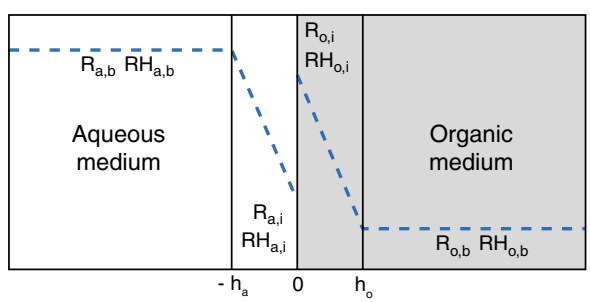

Figure 2. Schematic diagram of physical model with key parameters

DOI: 10.1002/bdd

aqueous diffusion layer, j_a, is given in Equation (1), where RH are R^- are the concentrations of non-ionized and ionized species, respectively, and D_a is the aqueous diffusion coefficient for both species.

$$j_a = -D_a \frac{d(RH)}{dx} - D_a \frac{d(R^-)}{dx} \quad (1)$$

Upon integration from x equal to $-h_a$ to zero (the thickness of the diffusion layer) the flux across the aqueous diffusion layer is given as a function of the concentration of drug species in the bulk, $R_{a,b}$, $RH_{a,b}$, and the concentration of drug species on the aqueous side of the interface, $R_{a,i}$, and $RH_{a,i}$, as shown in Equation (2).

$$j_a = \frac{D_a}{h_a}\left[\left(R_{a,b} + RH_{a,b}\right) - \left(R_{a,i} + RH_{a,i}\right)\right] \quad (2)$$

Using the same assumptions as above, the flux of drug from the organic side of the interface to the bulk organic phase can be defined in an analogous manner to Equation (1). It is not assumed that only non-ionized drug partitions into the organic medium, allowing for cases when ionized drug may form complexes with counterions and partition into the organic medium, for example (and the model does not change whether or not this assumption is made) [15]. Upon integration from x equals 0 to h_o (the thickness of the organic diffusion layer), the flux of drug across the organic interface, j_o, is given by Equation (3), where $R_{o,i}$ and $RH_{o,i}$, are the concentrations of ionized and non-ionized drug on the organic side of the interface respectively, and $R_{o,b}$ and $RH_{o,b}$ are the concentrations of ionized and non-ionized drug in the bulk organic phase, respectively. D_o, is the drug diffusion coefficient in the organic phase.

$$j_o = \frac{D_o}{h_o}\left[\left(R_{o,i} + RH_{o,i}\right) - \left(R_{o,b} + RH_{o,b}\right)\right] \quad (3)$$

The concentration of drug on the organic side of the interface can be related to the concentration of drug on the aqueous side of the interface (assumption 6) using the apparent partition coefficient at the interface defined by Equation (4). If the aqueous buffer capacity is high enough to maintain a constant bulk pH during the experiment, then the aqueous surface pH is constant and is equal to the bulk pH, and K_{ap} surface is equal to K_{ap} bulk.

$$K_{ap} = \frac{RH_{o,i} + R_{o,i}}{RH_{a,i} + R_{a,i}} \quad (4)$$

Using the pseudo-steady-state approximation (assumption 5) and assuming instantaneous transfer across the interface (assumption 7), the fluxes across the aqueous and organic diffusion layers can be set equal. Setting Equation (2) equal to Equation (3), eliminating $R_{o,i}$ and $RH_{o,i}$ using Equation (4), and letting C_a equal the total aqueous bulk drug concentration, $RH_{a,b} + R_{a,b}$, and C_o equal the total organic bulk drug concentration, $RH_{o,b} + R_{o,b}$, gives the pseudo-steady-state flux of drug as a function of the bulk aqueous and the bulk organic phase concentrations, shown in Equation (5).

$$j = \frac{D_o D_a K_{ap}}{\left[D_a h_o + D_o h_a K_{ap}\right]}\left[C_a - \frac{C_o}{K_{ap}}\right] \quad (5)$$

The interface permeation rate, P_I, across the aqueous and organic diffusion layers (barriers in series) defined by Equation (6) allows for further simplification of the total flux from the bulk aqueous to the bulk organic phase as shown in Equation (7). P_I can also be described in terms of the mass transfer coefficient across the organic diffusion layer, k_{org}, and the mass transfer coefficient across the aqueous diffusion layer, k_{aq}, according to Equation (8), where $k_{org} = D_o/h_o$ and $k_{aq} = D_a/h_a$.

$$\frac{1}{P_I} = \frac{h_o}{D_o K_{ap}} + \frac{h_a}{D_a} \quad (6)$$

$$j = P_I\left[C_a - \frac{C_o}{K_{ap}}\right] \quad (7)$$

$$\frac{1}{P_I} = \frac{1}{k_{org} K_{ap}} + \frac{1}{k_{aq}} \quad (8)$$

Equation (6) can be further simplified by relating D_o to D_a through the viscosities of the aqueous and organic media. According to the Hayduk and Laudie (HL) and Othmer and Thakar (OT) methods of estimating diffusion coefficient [16,17], the diffusion coefficient is a function of the molal

DOI: 10.1002/bdd

volume of the drug and the liquid viscosity. Using the HL method, D_o can be related to D_a according to Equation (9). When 1-octanol is used as the organic medium, assuming the viscosity of the aqueous buffer is 0.6915 cP (viscosity of water) and the viscosity of 1-octanol is 4.84 cP at 37 °C [18,19], then D_o is about equal to 0.11D_a.[1]

$$\frac{D_o}{D_a} \approx \left(\frac{\mu_a}{\mu_o}\right)^{1.14} \tag{9}$$

If it is assumed that h_a and h_o are equal, then the equation for P_I simplifies to Equation (10). h_a and h_o depend on factors such as liquid viscosity, stirring rate, agitator length and design, and vessel geometry. In reality, h_o is probably somewhat larger than h_a due to the higher viscosity of the organic medium (assuming similar rotational speeds and impeller geometries). However, the value of these simplifying assumptions is evident from Equation (10). When K_{ap} is greater than about 10, P_I is primarily determined by the aqueous diffusion layer permeability (or mass transfer coefficient, k_{aq}) since the organic phase is effectively functioning as a sink for the partitioning drug.

$$P_I \approx \frac{D_a}{h_a}\left(\frac{K_{ap}}{9.1 + K_{ap}}\right) \tag{10}$$

The time-dependent concentration of drug in the aqueous medium can be expressed according to Equation (11) since mass transfer only occurs through the interface and drug is not generated or destroyed in the system (assumptions 8 and 9). A_I is the surface area of the aqueous–organic interface, and V_a is the volume of aqueous medium. Equation (7) can be substituted into Equation (11) to give Equation (12). The aqueous and organic concentrations and K_{ap} are given the subscript, t, to indicate their time dependence. As stated previously, if the buffer capacity is high enough, then K_{ap} is not time dependent.

[1]D_o is equal to ~0.12D_a according to the OT method. The Wilke-Chang method gives diffusion coefficient as a function of an association parameter and liquid molecular weight in addition to liquid temperature and viscosity, and would estimate that D_o is equal to ~0.54D_a.

$$\frac{dC_a}{dt} = -\frac{A_I}{V_a} j \tag{11}$$

$$\frac{dC_a}{dt} = -\frac{A_I}{V_a} P_I \left[C_{a,t} - \frac{C_{o,t}}{K_{ap,t}}\right] \tag{12}$$

Before integrating Equation (12), $C_{o,t}$ must be related to $C_{a,t}$ using mass balance. Using assumptions 4 and 9 we can write Equation (13), where M_T is the total amount of drug in the system and V_o is the volume of organic medium.

$$M_T = C_{a,t} V_a + C_{o,t} V_o \tag{13}$$

Since, experimentally, the initial bolus of drug is injected into the aqueous phase at time 0, $C_{a,t=0}$ is equal to M_T. Integrating Equation (12) using this initial condition gives an expression for $C_{a,t}$ as a function of time, as shown in Equations (14), (15). Using the mass balance in Equation (13) allows determination of the concentration of drug in the organic phase as a function of time, which is given in Equation (16). Equations (17) and (18) give the fraction of drug in the aqueous and organic phases as a function of time, respectively.

$$C_{a,t} = \frac{M_T}{V_a(1+\beta)}\left[e^{-\frac{A_I}{V_a}P_I(1+\beta)t} + \beta\right] \tag{14}$$

$$\beta = \frac{V_a}{K_{ap} V_o} \tag{15}$$

$$C_{o,t} = \frac{M_T}{V_o(1+\beta)}\left[1 - e^{-\frac{A_I}{V_a}P_I(1+\beta)t}\right] \tag{16}$$

$$F_{a,t} = \frac{1}{(1+\beta)}\left[e^{-\frac{A_I}{V_a}P_I(1+\beta)t} + \beta\right] \tag{17}$$

$$F_{o,t} = \frac{1}{(1+\beta)}\left[1 - e^{-\frac{A_I}{V_a}P_I(1+\beta)t}\right] \tag{18}$$

The value of β (defined in Equation (15)) is the volume ratio of aqueous to organic media normalized by the apparent partition coefficient, K_{ap}, and it impacts the rate of partitioning into the organic medium and the fraction of drug in each phase at equilibrium. As the normalized organic volume (K_{ap}*V_o) increases, such as for drugs with high partition coefficients, the value of β decreases towards zero. The rate of partitioning is reflected

DOI: 10.1002/bdd

in the decay constant, which is equal to (1+ β)* (A_I/V_a)*P_I. The fraction of the dose in the organic medium at equilibrium, $F_{o,\infty}$, is equal to $1/(1+\beta)$. When β is less than about 0.1, Equations (14) and (16)–(18) can be simplified to Equations (19)–(22), since the predicted concentration or fraction of drug in each phase at any given time is within 10% of the value predicted using the full equations.

The exponential decay Equations (19)–(20) are the integrated solutions to first-order ordinary differential equations with respect to concentration or fraction in the aqueous phase, respectively. Equations (21)–(22) are analogous to first-order absorption equations prevalent in pharmacokinetic modeling. The decay constant, k_p, which is equal to (A_I/V_a)*P_I, can be compared directly with the pharmacokinetic first-order 'absorption rate constant', k_a, since the equations are analogous.

$$C_{a,t} = \frac{M_t}{V_a} e^{-\frac{A_I}{V_a} P_I t} = \frac{M_t}{V_a} e^{-k_p t} \tag{19}$$

$$F_{a,t} = e^{-\frac{A_I}{V_a} P_I t} = e^{-k_p t} \tag{20}$$

$$C_{o,t} = \frac{M_T}{V_o}\left[1 - e^{-\frac{A_I}{V_a} P_I t}\right] = \frac{M_T}{V_o}\left[1 - e^{-k_p t}\right] \tag{21}$$

$$F_{o,t} = 1 - e^{-\frac{A_I}{V_a} P_I t} = 1 - e^{-k_p t} \tag{22}$$

Materials

Ibuprofen (Albermarle Lot No. 2050-0032F for experiments 1–4, and Sigma Aldrich, Cat No. I4883-10G for experiments 5–10), nimesulide (Sigma Aldrich, Cat No. 1016-25G) and piroxicam (Sigma Aldrich, Cat No. P0847-10G) powder, as well as 1-octanol (99% purity) and HPLC-grade methanol, were purchased commercially. The relevant material properties are included in Table 1.

Apparent partition coefficient

The K_{ap} of piroxicam at 37 °C in pH 7.4 buffer was determined. Ten mg of drug was added to a glass vial containing 7 ml of 50 mM pH 7.4 sodium phosphate buffer and 7 ml of 1-octanol. The glass vial was placed in an incubator shaker at 37 °C and 150 rpm and allowed to shake for 2 days, after which two samples were removed from each phase and prepared for concentration analysis using UV. Absorbance was measured at 340 nm for the 1-octanol phase and 356 nm for the aqueous phase.

Table 1. Properties of the model drugs

Drug	Ibuprofen	Nimesulide	Piroxicam
BCS class	II	II	II
Structure	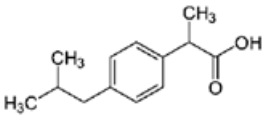	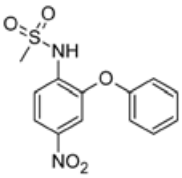	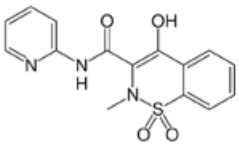
Molecular weight (g/mol)	206.3	308.3	331.3
pK_a at 37 °C	4.4 (acidic)[a]	6.8 (acidic)[b]	2.3 (basic)[c] 5.3 (acidic)[c]
cLog *P*	3.84[d]	1.79[d]	0.60[d]
Log *D*	pH 4.5–3.4[e] pH 5.0–3.1[e] pH 6.5–1.7[e] pH 6.8–1.4[e] pH 7.5–0.7[e]	pH 1.2: 1.92[f] pH 7.5: -0.10[e]	pH 1.2: 0.92[f] pH 7.5: 0.8[g]
Intrinsic solubility at 37 °C (M)	3.3×10^{-4}[a]	3.8×10^{-5}[f]	6.6×10^{-5}[f]

[a]Measured value from reference [40].
[b]Calculated value from reference [30].
[c]Measured value from reference [41].
[d]Calculated value from reference [26].
[e]Calculated using a pK_a of 4.4 and a Log *P* of 3.8, assuming only non-ionized drug partitions into 1-octanol.
[f]Measured value from reference [12].
[g]Measured value from reference [27].

DOI: 10.1002/bdd

The K_{ap} of ibuprofen at 37 °C in pH 7.5 was measured. Either 50 ml or 100 ml (preparation 1 or 2, respectively) of a 511 μg/ml solution of ibuprofen in 1-octanol saturated with 50 mM sodium phosphate buffer (pH 7.5) was added to either 75 ml or 150 ml (preparation 1 or 2, respectively) of 50 mM sodium phosphate buffer (pH 7.5) saturated with 1-octanol, and the mixture was stirred vigorously overnight at 37 °C.

The media were allowed to separate for half a day and two samples were removed from both phases and prepared for concentration analysis via UV. The absorbance was measured at 274 nm for the 1-octanol samples and 221 nm for the aqueous samples.

The K_{ap} of ibuprofen at 37 °C in pH 1.2 buffer was measured. Seventy-five ml of a solution of 1-octanol containing 15.6 mg/ml ibuprofen saturated with 65 mM HCl and 50 ml of 65 mM HCl saturated with 1-octanol was added to a 37 °C vessel and stirred vigorously overnight (two preparations were made). The media were allowed to separate for half a day and two samples were removed from both phases and prepared for concentration analysis via UV. The second derivative of the absorbance was measured at 284 nm for the 1-octanol samples and 237 nm for the aqueous samples.

For each analysis K_{ap} was determined by calculating the ratio of the concentration of drug in the 1-octanol to the concentration of drug in the aqueous medium at equilibrium.

In vitro partitioning experiments

In vitro partitioning experiments were performed to test the validity of the model. Experiments were conducted using BCS II model compounds ibuprofen, nimesulide and piroxicam in three different types of two-phase dissolution apparatuses, in two different laboratories, by three different researchers. As all three model compounds are at least partially ionized within the physiological pH, experiments were conducted across a pH range to test the effect of apparent partition coefficient on the model. 1-Octanol was used as the organic medium in all cases. Different volumes of buffer (150, 250 ml), different volumes of 1-octanol (150, 200, 250 ml), different impeller rotational speeds (40, 50, 75, 77 rpm), different pHs and different doses (2.5, 3.75, 4, 5, 6.25, 12.5, 15.0 mg) were used for the experiments. Details for each experiment are given in Table 2. Apparatus 1 was a 9 cm diameter jacketed glass vessel with a flat bottom. This apparatus utilized a dual paddle, which consisted of two identical 5 cm diameter paddles, which were centred vertically in each phase.

Apparatus 2 consisted of a USP 2 vessel with a diameter of 9.8 cm, and the paddle was mounted such that the bottom of the compendial paddle was approximately 2.5 cm from the bottom of the vessel and the additional paddle was centred vertically in the 1-octanol. Apparatus 3 was a USP 2 apparatus (1000 ml with a hemispherical bottom), which utilized a dual paddle consisting of an additional paddle (5 cm diameter) mounted on the regular compendial paddle, with a vessel diameter of 10.1 cm. The compendial paddle was mounted such that the bottom of the paddle was approximately 2 mm from the bottom of the vessel, and the additional paddle was mounted such that it was centred vertically in the 1-octanol.

For all experiments the buffer solution was made up and mixed overnight with 1-octanol in a 1:1 ratio at 37 °C. The solutions were separated using a separatory funnel and stored at 37 °C before and between partitioning runs. The pH of the buffer saturated with 1-octanol was measured using a calibrated pH meter. The pH was adjusted using concentrated HCl or NaOH solution as necessary to bring it to the desired pH. The appropriate volumes of buffer saturated with 1-octanol and 1-octanol saturated with buffer were then measured using a graduated cylinder and added to the dissolution vessel, which was heated to 37 ± 0.2 °C using a water bath. The phases were stirred at the desired rotational speed for at least 20 min prior to the beginning of the run. Prior to starting the run, the temperature was measured with an external thermometer. At the start of the experiment, drug in solution was injected into the aqueous buffer. The concentration in each phase was measured as a function of time until a plateau was reached in each phase (in most cases). In all cases, calibrated, UV Fiber Optic Probes (StellarNet Inc. Black Comet, Tampa, Florida for Apparatus 1 and 3, or Pion Rainbow, Billerca, MA for Apparatus 2) were mounted such that

DOI: 10.1002/bdd

Table 2. Experimental details for *in vitro* partitioning experiments

Exp./Fig No.	Apparatus	Drug	pH	Buffer species[a]	Buffer Conc. mM	Rotational speed rpm	V_a ml	V_o ml	M_T mg	A_I[b] cm^2	β	M_T/V_a μg/ml	A_I/V_a cm^{-1}	No. rep.[c]
3/3(a)	1	Ibuprofen	1.5	HCl	10	77	150	150	2.5	63.6	1.58×10^{-4}	16.7	0.42	2
4/3(b)	1	Ibuprofen	4.3	Sodium acetate	50	77	150	150	2.5	63.6	3.17×10^{-4}	16.7	0.42	2
5/3(c)	1	Ibuprofen	4.4	Sodium acetate	50	77	150	150	2.5	63.6	2.84×10^{-4}	16.7	0.42	2
6/3(d)	1	Ibuprofen	6.3	Sodium phosphate	43	77	150	150	2.5	63.6	1.28×10^{-2}	16.7	0.42	2
7/4(a)	2	Ibuprofen	5	Sodium acetate	50	75	250	200	6.25	75.4	9.87×10^{-4}	25	0.3	3
8/4(b)	2	Ibuprofen	6.8	Sodium phosphate	50	75	250	200	12.5	75.4	5.00×10^{-2}	50	0.3	3
9/4(c)	2	Ibuprofen	6.8	Sodium phosphate	50	75	250	200	6.25	75.4	5.00×10^{-2}	25	0.3	3
10/4(d)	2	Ibuprofen	6.8	Sodium phosphate	50	40	250	200	6.25	75.4	5.00×10^{-2}	25	0.3	3
11/4(e)	2	Ibuprofen	7.5	Sodium phosphate	50	75	250	200	6.25	75.4	0.144	25	0.3	3
12/4(f)	2	Ibuprofen	7.5	Sodium phosphate	50	40	250	200	6.25	75.4	0.144	25	0.3	3
13/4(g)	3	Ibuprofen	4.5	Sodium acetate	50	50	250	250	4	80.1	3.58×10^{-4}	16	0.32	3
14/5(a)	2	Piroxicam	1.2	HCl	0.06	75	250	200	15	75.4	0.149	60	0.3	3
15/5(b)	2	Piroxicam	1.2	HCl	0.06	75	250	200	5	75.4	0.149	20	0.3	3
16/5(c)	2	Piroxicam	1.2	HCl	0.06	75	250	200	3.75	75.4	0.149	15	0.3	3
17/5(d)	2	Piroxicam	7.5	Sodium phosphate	50	40	250	200	5	75.4	2.53	20	0.3	3
18/5(e)	2	Piroxicam	7.5	Sodium phosphate	50	75	250	200	5	75.4	2.53	20	0.3	3
19/5(f)	2	Piroxicam	7.5	Sodium phosphate	50	75	250	200	15	75.4	2.53	60	0.3	3
20/5(g)	2	Nimesulide	7.5	Sodium phosphate	50	75	250	200	12.25	75.4	8.99×10^{-2}	49	0.3	3

[a]Buffers used in experiments 3–13 were made isotonic with bodily fluids.
[b]A_I in experiments conducted at 75 rpm in Apparatus 2 may have been as much as 4% higher than reported due to a slight vortex observed during mixing.
[c]Number of replicates performed per experimental condition.

DOI: 10.1002/bdd

one collected absorbance data in the aqueous medium and/or one collected absorbance data in the 1-octanol as a function of time. For ibuprofen in Apparatus 1 and 3, the difference between the absorbance at 222 nm and 375 nm was correlated to concentration in either the aqueous or organic medium using standard solutions. For Apparatus 2, the absorbance of ibuprofen at 222 nm (aqueous and 1-octanol for all pHs), piroxicam at 336 or 356 nm (aqueous at pH 1.2 or 7.5) and nimesulide at 300 or 390 nm (aqueous at pH 1.2 or aqueous and 1-octanol at pH 7.5) were correlated to the concentration using standard solutions. Experiments were run in duplicate or triplicate for each condition.

Data analysis

The fraction of the dose in the aqueous buffer and/or 1-octanol was plotted as a function of time. The full model (Equation (17)) for the fraction of the drug in the buffer was fit to the buffer data and the full model (Equation (18)) for the fraction of the drug in the organic phase was fit to the 1-octanol data for each experiment using non-linear least squares regression with the Nelder-Mead simplex algorithm as the optimization method using Python™, Software (Python Foundation, Wolfeboro Falls, NH). P_I was the only adjustable parameter in the analysis. The value of β was calculated using a measured value of K_{ap} when available, but was otherwise calculated using an estimated value of K_{ap}, which was calculated assuming only non-ionized drug partitions into 1-octanol. Fitted values and 95% confidence intervals for P_I for each experimental condition were reported. If both buffer and 1-octanol data for a single condition were available, a single, best-fit P_I was determined. The average h_a for each experiment was estimated using Equation (10).

The model was also fit to experimental two-phase partitioning data generated by Grassi *et al*. [12]. Numerical values for the fraction of the dose in the aqueous phase as a function of time were determined by carefully extracting the average concentration at each time point from concentration–time plots using the ruler tool in Adobe® Photoshop® CS3 (Adobe, San Jose, CA) and dividing by the dose.

Results

Apparent partition coefficient

The measured apparent partition coefficients for ibuprofen at pH 1.2 and pH 7.5 were 6670.5 (7.9% relative standard deviation (RSD)), and 8.7 (3.7% RSD), respectively. The measured apparent partition coefficient for piroxicam at pH 7.4 was 0.49 (2.0% RSD).

In vitro experiments

Plots of experimental fraction of drug in aqueous buffer and/or 1-octanol as a function of time along with model fits using the best fit P_I value are included in Figures 3–6. The best fit P_I and h_a values for each experimental condition are included in Table 3.

Discussion

Comparison of mechanistic analysis to kinetic models

A few researchers have introduced kinetic models to describe aqueous-to-organic phase partitioning [13,20]. In 2002 Grassi, Coceani and Magarotto published a comprehensive mathematical model describing the partitioning kinetics of a solute from an aqueous to an organic medium [12]. They proposed a steady-state differential rate equation for aqueous drug concentration as a function of rate constants for transfer from the aqueous to the organic (k_{wo}) and from the organic to aqueous (k_{ow}) phases. Their solution for aqueous concentration, C_w, as a function of time is shown in Equation (23), where M_o is the total mass of dissolved drug in the system, V_w and V_o are the volumes of the aqueous and organic phases, respectively, and A is the surface area of the interface. Upon inspection, one can see that Equation (23) is analogous to Equation (14) of our mechanistic model if one sets k_{ow} equal to P_I/K_{ap} and k_{wo} equal to P_I.

$$C_w = \frac{k_{ow}M_o}{k_{wo}V_o + k_{ow}V_w} - \left(\frac{k_{ow}M_o}{k_{wo}V_o + k_{ow}V_w} - C_{wi}\right)e^{-\left(A\frac{k_{wo}V_o + k_{ow}V_w}{V_oV_w}\right)} \tag{23}$$

DOI: 10.1002/bdd

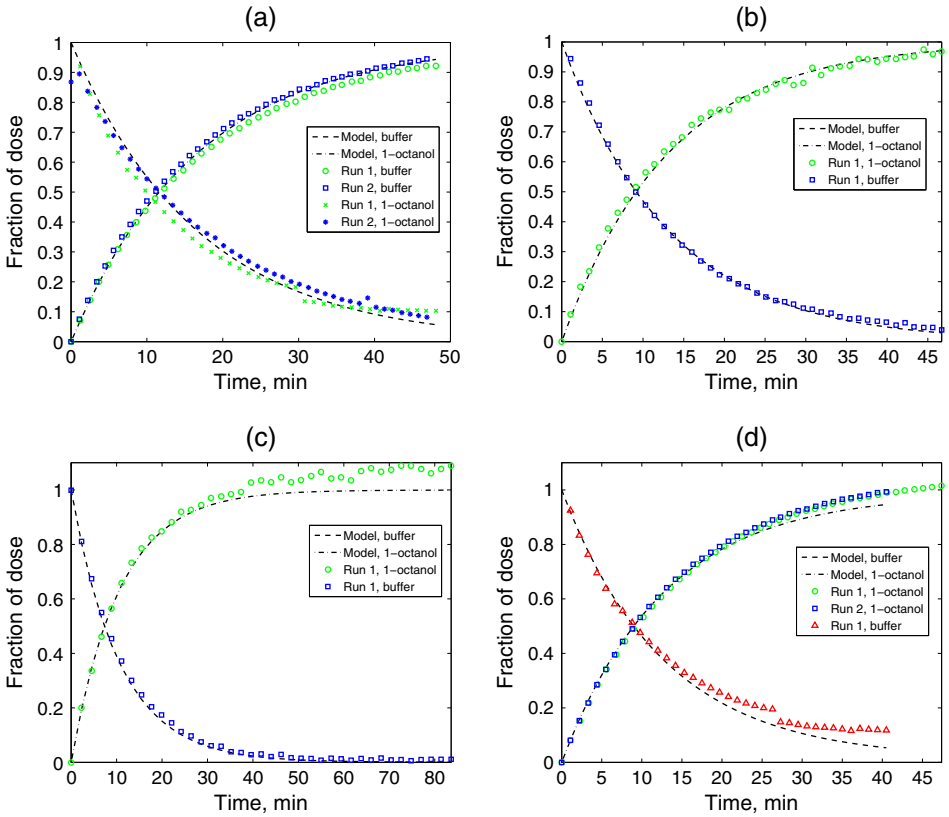

Figure 3. *In vitro* fraction of dose as a function of time for ibuprofen in Apparatus 1 (experiments 3–6 in plots (a)–(d), respectively, see also Table 3)

Grassi *et al*. state that Equation (23) cannot be applied to partitioning of 'sparingly soluble drugs in one or both phases' and propose an empirical modification resulting in four different equations for C_w as a function of time. They select the proper equation based upon the values of defined model parameters that are a function of both experimental and fitted parameters (k_{ow} and k_{wo}), which, according to their analysis cannot be determined *a priori*. When 'Case 3' of their model is satisfied ($a = 0$), their model simplifies to their original model (Equation (23)). Setting k_{ow} equal to P_I/K_{ap} and k_{wo} equal to P_I reveals that this occurs for cases when C_{so}/C_{sw} is close to or equal to K_{ap}, where C_{sw} is the equilibrium solubility of drug in the aqueous phase, and C_{so} is the equilibrium concentration of drug in the organic phase. For the majority of small molecular compounds, $K_{ap} \sim C_{so}/C_{sw}$, assuming the effect of organic/aqueous mutual saturation on the K_{ap} is small, and phenomenon such as micellization or self-association are not occurring [21,22]. If C_{so} and C_{sw} are measured in mutually saturated organic medium and aqueous medium respectively, then K_{ap} should be equal to $C_{so}/C_{s,}$ and Equation (23) of the Grassi model (which is equivalent to Equation (14) our model) should be adequate in describing the partitioning kinetics of the majority of drugs of pharmaceutical interest.

An advantage of our model over existing kinetic models is that all model parameters are defined by the experimental set up, can be measured or calculated, or can be estimated *a priori*. The values of M_T, V_a, V_o and A_I are defined by the experimental set up. K_{ap} can be measured using established methods or can be estimated using molecular descriptors [15,23,24]. P_I is a function of K_{ap}, D_a, D_o, h_a and h_o. As D_a and D_o can be estimated, the only unknown parameters are h_a and h_o [16], and when K_{ap} is sufficiently large, P_I is simply a function of D_a and h_a, which simplifies estimation

DOI: 10.1002/bdd

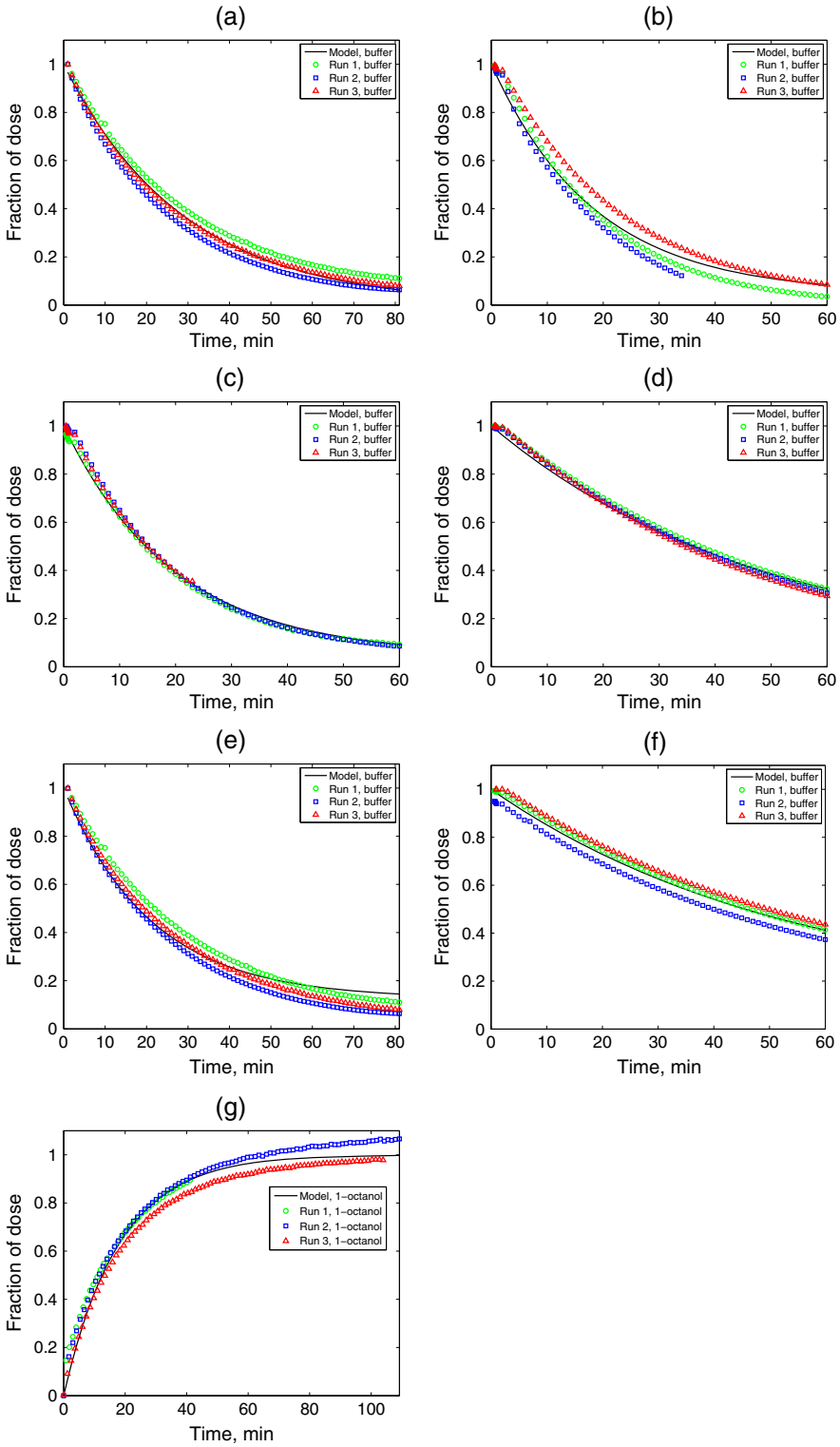

Figure 4. *In vitro* fraction of dose as a function of time for ibuprofen in Apparatus 2 and 3 (experiments 7–13 in plots (a)–(g), respectively, see also Table 3)

DOI: 10.1002/bdd

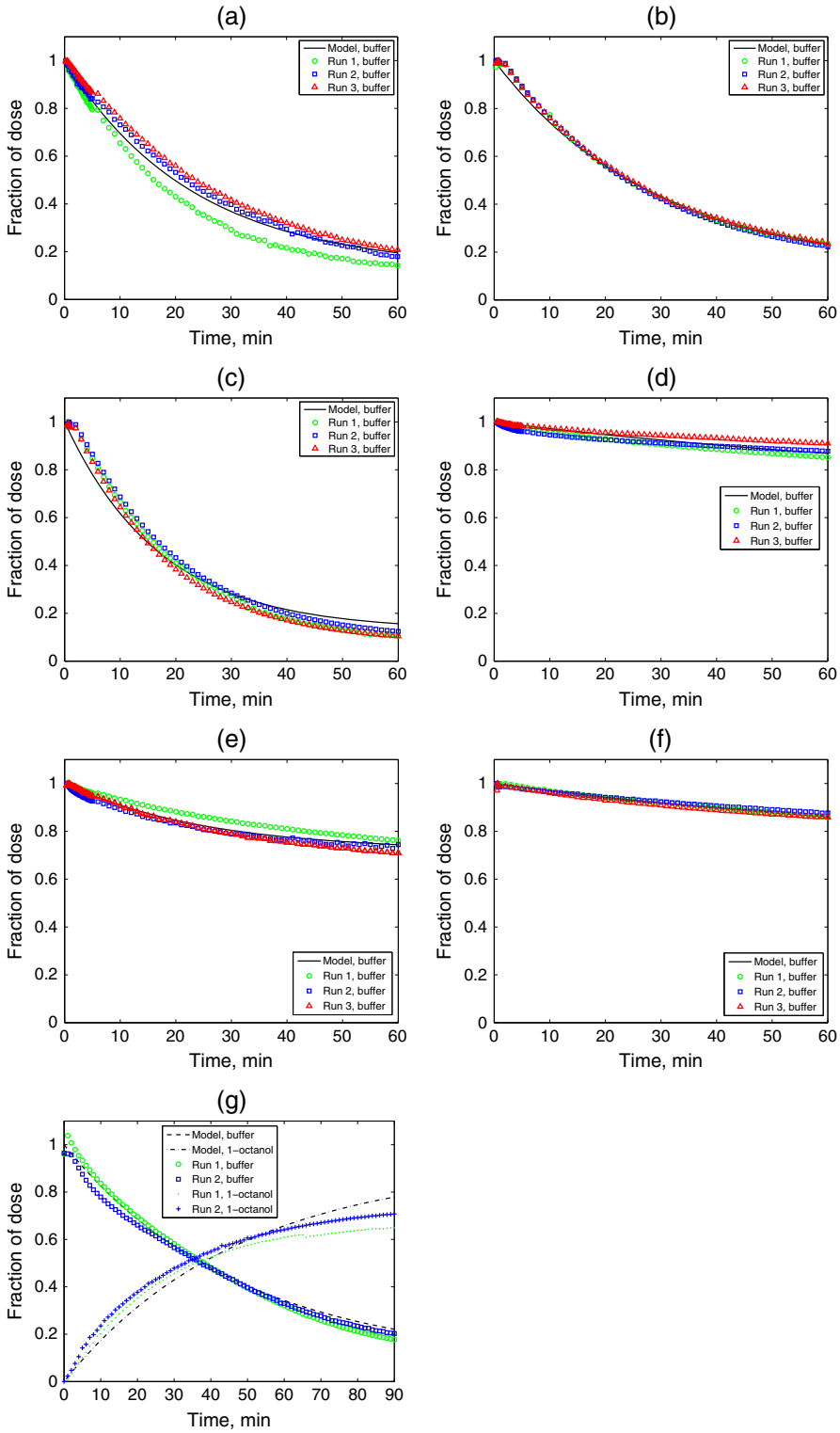

Figure 5. *In vitro* fraction of dose as a function of time for piroxicam and nimesulide in Apparatus 2 (experiments 14–20 in plots (a)–(g), respectively, see also Table 3)

DOI: 10.1002/bdd

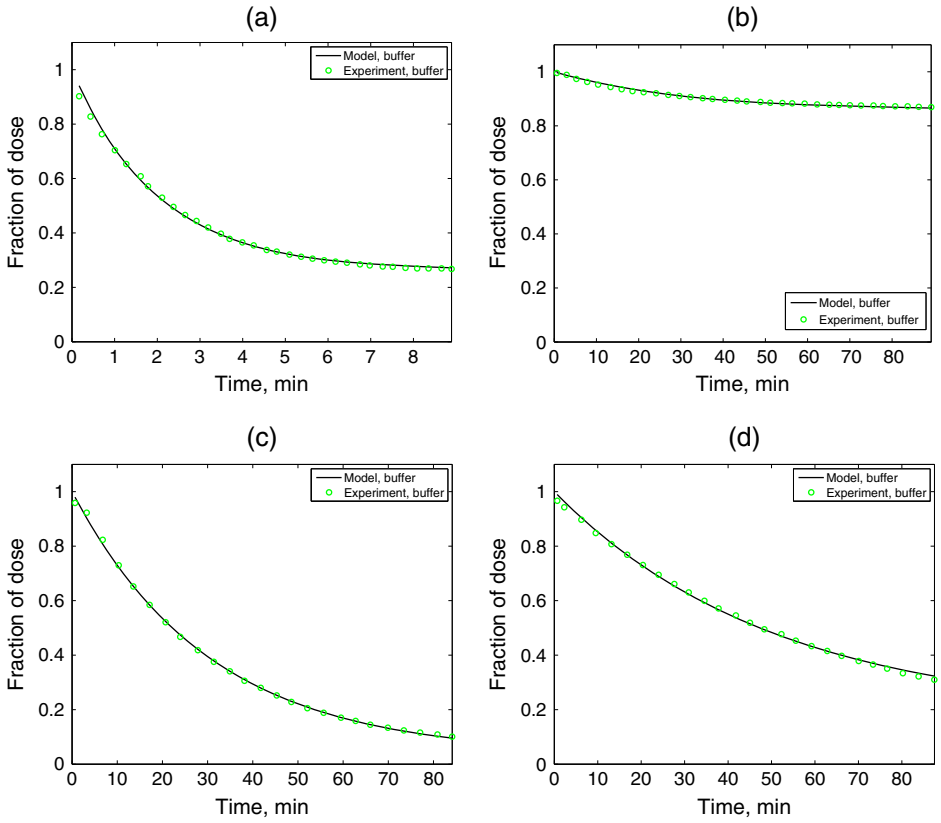

Figure 6. *In vitro* fraction of dose as a function of time for piroxicam and nimesulide in Grassi *et al.*'s experiments (experiments 21–24 in plots (a)–(d), respectively, see also Table 3)

of P_I. Alternatively, P_I can be easily determined experimentally in the two-phase system as has been done for other systems such as Caco-2 [25].

Apparent partition coefficient

The partition coefficient of ibuprofen at pH 1.2 (drug is 100% unionized) of 6670.5 (Log *P* of 3.82) is in close agreement with the calculated Log *P* value of 3.84 [26]. The measured apparent partition coefficient of ibuprofen of 8.7 at pH 7.5 is about 40% higher than the estimated value of 5.2, which was calculated assuming only non-ionized drug partitions into the 1-octanol (using a pK_a of 4.4 and the measured partition coefficient of the non-ionized drug at pH 1.2). The apparent partition coefficient of piroxicam of 0.49 at pH 7.4 is relatively close to the value of 0.8 at pH 7.5 determined by Yazdanian *et al.*, which was also determined at 37 °C [27].

In vitro partitioning experiments

The model fit the data quite well in all cases. Deviations from the model are likely due to errors in the analytical method and/or suboptimal estimates for K_{ap}. As demonstrated in Figures 3–6, the fraction of dose versus time curves for each run deviated slightly. These deviations are not surprising, as analytical error was noted when taking absorbance readings of mutually saturated solvents at elevated temperatures. In addition, using measured rather than calculated values for K_{ap} for ibuprofen at pH 4.3, 4.4, 4.5, 6.3, and 6.8, and using a measured value for piroxicam at pH 7.5 rather than pH 7.4 may have given better estimates for P_I in these experiments.

Based on the mass transport analysis, when β is less than about 0.1 the organic diffusion layer should cause negligible diffusional resistance, and the value of P_I should be primarily a function

DOI: 10.1002/bdd

Table 3. Best fit P_I and estimated h_a values from *in vitro* partitioning experiments

Exp./Fig No.	Drug	Apparatus	pH	Rotational speed rpm	A/V_a cm^{-1}	β	M_T/V_a μg/ml	$F_{o,\ inf}$	$K_{ap}/(9.2+K_{ap})$	$P_I \times 10^4$ cm/s × 10^4	(95% CI)	h_a, full μm	(95% CI)
3/3(a)	Ibuprofen	1	1.5	77	0.42	1.58×10^{-4}	16.7	1.00	1.00	23.71	(22.16–25.41)	32	(29–34)
4/3(b)	Ibuprofen	1	4.3	77	0.42	2.84×10^{-4}	16.7	1.00	1.00	30.06	(29.45–30.68)	25	(24–25)
5/3(c)	Ibuprofen	1	4.4	77	0.42	3.17×10^{-4}	16.7	1.00	1.00	37.52	(30.30–47.73)	20	(16–25)
6/3(d)	Ibuprofen	1	6.3	77	0.42	1.28×10^{-2}	16.7	0.99	0.89	30.81	(28.79–33.03)	22	(20–23)
7/4(a)	Ibuprofen	2	5.0	75	0.30	9.87×10^{-4}	25.0	1.00	0.99	19.08	(18.13–20.10)	39	(37–41)
8/4(b)	Ibuprofen	2	6.8	75	0.30	5.00×10^{-2}	50.0	0.95	0.73	28.73	(24.64–33.73)	19	(16–22)
9/4(c)	Ibuprofen	2	6.8	75	0.30	5.0×10^{-2}	25.0	0.95	0.73	26.85	(26.09–27.63)	20	(20–21)
10/4(d)	Ibuprofen	2	6.8	40	0.30	5.00×10^{-2}	25.0	0.95	0.73	10.92	(10.69–11.17)	50	(49–51)
11/4(e)	Ibuprofen	2	7.5	75	0.30	1.44×10^{-1}	25.0	0.87	0.49	23.01	(20.07–26.59)	16	(14–18)
12/4(f)	Ibuprofen	2	7.5	40	0.30	1.44×10^{-1}	25.0	0.87	0.49	9.03	(8.38–9.70)	40	(38–43)
13/4(g)	Ibuprofen	3	4.5	50	0.32	3.58×10^{-4}	16.0	1.00	1.00	28.72	(25.45–32.65)	26	(23–29)
14/5(a)	Piroxicam	2	1.2	75	0.30	1.49×10^{-1}	15.0	0.87	0.48	20.85	(16.47–26.73)	15	(12–19)
15/5(b)	Piroxicam	2	1.2	75	0.30	1.49×10^{-1}	20.0	0.87	0.48	17.06	(16.77–17.36)	19	(18–19)
16/5(c)	Piroxicam	2	1.2	75	0.30	1.49×10^{-1}	60.0	0.87	0.48	28.04	(24.65–32.12)	11	(10–13)
17/5(d)	Piroxicam	2	7.5	40	0.30	2.53	20.0	0.28	0.05	1.64	(1.48–1.80)	21	(19–23)
18/5(e)	Piroxicam	2	7.5	75	0.30	2.53	20.0	0.28	0.05	6.15	(5.87–6.44)	6	(5–6)
19/5(f)	Piroxicam	2	7.5	75	0.30	2.53	60.0	0.28	0.05	1.78	(1.75–1.81)	19	(19–20)
20/5(g)	Nimesulide	2	7.5	75	0.30	8.99×10^{-2}	49.0	0.92	0.60	10.71	(9.80–11.71)	39	(36–43)
21/6(a)	Piroxicam	Grassi	1.2	Unknown	0.23	0.357	15.2	0.74	0.48	265.4	(257.7–273.5)	12	(12–12)
22/6(b)	Piroxicam	Grassi	7.5	Unknown	0.23	6.07	21.8	0.14	0.05	3.41	(3.35–3.46)	10	(10–10)
23/6(c)	Nimesulide	Grassi	1.2	Unknown	0.23	3.59×10^{-2}	8.5	0.97	0.90	22.98	(22.71–23.25)	27	(27–28)
24/6(d)	Nimesulide	Grassi	7.5	Unknown	0.23	2.16×10^{-1}	45.0	0.82	0.60	11.80	(11.60–12.01)	36	(35–36)

DOI: 10.1002/bdd

of D_a and h_a. Therefore, experiments 3–6 conducted with ibuprofen in Apparatus 1 are predicted to have similar P_I values (β was less than or equal to 0.01 for all conditions). While P_I values were similar between pH 4.3 and 6.3, P_I was somewhat smaller at pH 1.5. The best-fit P_I value for all conditions was 3.0×10^{-3} (range of 2.2–4.8×10^{-3}) cm/s. Since the contribution of the organic diffusion layer is expected to be small, h_a values calculated from these experiments should be reasonably accurate. The best-fit value across all conditions was 25 (range of 16–34) μm, which is in the range of 10–50 μm that was hypothesized *a priori* to be a practical range. Ibuprofen partitioning in Apparatus 2 (Exp. 7) and 3 (Exp. 13) at pH values low enough to assume negligible organic diffusional resistance was also measured. Estimated h_a values were 39 (37–41) μm and 26 (23–29) μm, respectively in these systems. As with Apparatus 1, the values fall within the expected range. Comparisons between h_a in the different apparatuses cannot easily be made due to the different geometries and rotational speeds. When β is not less than 0.1, P_I should increase with increasing K_{ap}. The expected trend was observed for ibuprofen in Apparatus 2 (compare experiments 10 and 12 and experiments 9 and 11), Piroxicam in Apparatus 2 (compare experiments 15 and 18 and experiments 16 and 19), Piroxicam in Grassi *et al.*'s work (compare experiments 21 and 22) and nimesulide in Grassi *et al.*'s work (compare experiments 23 and 24).

Since an increase in impeller rotational speed should act to decrease the thickness of the aqueous and organic diffusion layers, P_I should increase with increasing rotational speed. This trend was observed in all experiments in which it was tested. For ibuprofen in Apparatus 2, a two-fold increase in impeller rotational speed led to a two-and-a-half-fold increase in P_I at both pH 6.8 (compare experiments 9 and 10) and pH 7.5 (compare experiments 11 and 12). For piroxicam in Apparatus 2, a two-fold increase in rotational speed led to about a six-and-a-half fold increase in P_I (compare experiments 17 and 18). This result may be occurring due to the smaller K_{ap} of piroxicam at pH 7.5 (~0.49) compared with ibuprofen at pH 6.8 (~25.0) or pH 7.5 (8.7). When K_{ap} is large, although an increase in rotational speed decreases both h_a and h_o, the contribution of h_o to P_I is minimal. However, when K_{ap} is small, the values of both h_a and h_o have an effect on the value of P_I. For instance, assuming h_a and h_o are equal, and $D_o = 0.11\ D_a$ (valid for a system of buffer and 1-octanol at 37 °C), when K_{ap} is between 10 and 20, the contributions of h_a and h_o on P_I are about equal. However, when K_{ap} is 0.5, the contribution of h_o is about 20 times that of h_a.

The value of M_T/V_a is not expected to have an effect on P_I. A small difference (~7%) between P_I values was observed for ibuprofen at pH 6.8 in Apparatus 2 (compare experiments 8 and 9). More significant differences were observed for piroxicam in Apparatus 2 at pH 1.2 (compare experiments 14, 15 and 16), for which P_I values differed by anywhere between about 14% and 64%, and piroxicam in Apparatus 2 at pH 7.5 (compare experiments 18 and 19), for which values differed by about 73% and 275%. M_T/V_a and P_I. Since there was no trend between an increase in M_T/V_a and P_I, and because the concentration of drug in the aqueous medium was far from saturation for all experiments (≤ 0.3% for ibuprofen at pH 6.8, ≤ 24% for piroxicam at pH 1.2, and ≤ 3% for piroxicam at pH 7.5.[2]) the unexpected impact of M_T/V_a on P_I may be due to experimental error. As can be observed by examining Figures 3–6, replicate runs at each condition varied in some cases, and the shapes of the experimental curves sometimes deviated slightly from the predicted curves.

Scaling parameters for ensuring physiological relevance

To maintain the physiological relevance of the two-phase system, $C_{a,t}$ *in vitro* should be maintained close to $C_{a,t}$ *in vivo*. Maintaining a physiological $C_{a,t}$ is important for drugs with high dose numbers since C_a can be very close to C_s, and can thus have a large impact on both the dissolution and partitioning rates in these cases [3]. As A_I, V_a, P_I and M_T all influence $C_{a,t}$ in the two-phase system, they are important parameters to consider.

The partitioning rate coefficient, k_p, (equal to $(A_I/V_a)*P_I$) reflects the rate at which drug parti-

[2]The saturation solubility of Ibuprofen at pH 6.8 was estimated using the intrinsic solubility and pK_a values given in Table 1. The saturation solubilities of Piroxicam at pH 1.2 and pH 7.5 were taken from reference 12.

DOI: 10.1002/bdd

tions into the organic medium. Therefore, one approach to establish physiological relevance is to keep the *in vitro* k_p equal to the expected absorption rate coefficient, k_a, *in vivo*. This approach assumes first-order absorption kinetics and a relatively high fraction absorbed *in vivo* (F_a). Using a known or estimated k_a and after measuring or estimating P_I, A_I/V_a can be adjusted such that k_p and k_a are similar according to Equation (24).

$$k_p = \left(\frac{A_I}{V_a} P_I\right)_{in\ vitro} = k_a = \left(\frac{A}{V} P_{eff}\right)_{in\ vivo} \quad (24)$$

While ideally V_a *in vitro* would be set equal to the intestinal liquid volume, V, *in vivo*, it is not necessary to do so for dissolution studies as long as M_T/V_a and dose/V are similar. The average total fasted intestinal volume *in vivo* is about 100 ml in humans, which may be contained within a number of liquid pockets [28]. Neglecting gastric emptying rate and assuming a bolus of dissolved drug in the intestine *in vivo*, M_T is equal to the dose. For more slowly releasing dosage forms, M_T is equal to the amount of dissolved drug, which depends on a number of factors. Thus, the simplest way to ensure physiological relevance of the *in vitro* dissolution test is to set M_T/V_a *in vitro* equal to dose/V (dose/100 ml in fasted humans).

Although k_a is not typically known *a priori* (especially for drugs early in development) it may be estimated. Several models exist for estimating *in vivo* k_a in humans for passively absorbed drugs [29]. The value of k_a can also be estimated using estimates of A/V and P_{eff}. P_{eff} in humans for passively absorbed drugs can be estimated using models that use molecular descriptors as input parameters [29,30], and it can also be estimated based on Caco-2 or rat perfusion studies [29]. While P_{eff} must be estimated for each drug, we propose using an average *in vivo* A/V to estimate k_a. Assuming the small intestine to be a perfect cylinder, Amidon *et al*. estimated A/V to be equal to $2/r$, where r is the radius of the small intestine [3]. Assuming a radius of 2 cm [5], this relationship would suggest an A/V of 1.0. However, as the human small intestine is a convoluted tube, it is likely that a compressed rather than a perfect cylindrical geometry would allow for a more accurate calculation of the geometrical surface area and A_I/V_a. Assuming a radius of 2 cm, a volume of 100 ml, and a constant perimeter, we calculated A_I/V_a based on percent compression, as shown in Table 4. While there is evidence that the liquid in the small intestine is not continuous, but instead is contained in multiple liquid pockets, for simplicity, our calculation method assumes that the compressed cylinder is completely full of liquid. Assuming the liquid contained in the liquid pockets assumes the shape of the intestine, our calculation method should be valid for discrete or continuous liquid since the surface area of each pocket would be additive. Literature values of total small intestinal length give an average of about 300 cm [5]. As shown in Table 4, zero percent compression (perfect cylinder) shows that 100 ml of liquid would fill 8 out of the 300 cm (assuming the liquid takes the shape of the intestine), while the 100 ml would reside in 19 out of the 300 cm if the intestine were 70% compressed.

Table 4. Calculated length, surface area, and surface-area-to-volume ratio, A_I/V_a, of a 100 ml cylinder as a function of percent compression assuming a constant perimeter

% compression	a[a] (cm)	b[b] (cm)	Length[c] (cm)	Surface area[d] (cm^2)	A_I/V_a[e] (cm^{-1})
95	0.1	2.8	112.6	1415.1	14.15
90	0.2	2.8	56.4	708.9	7.09
70	0.6	2.8	19.2	241.2	2.41
60	0.8	2.7	14.7	184.3	1.84
50	1.0	2.6	12.0	151.2	1.51
30	1.4	2.5	9.3	116.3	1.16
0	2.0	2.0	8.0	100.0	1.00

[a]Equal to average radius, r (equal to 2 cm), times (100% – % compression)/100%.
[b]Equal to $\sqrt{(r^2/0.5 - a^2)}$. Uses approximate formula for the perimeter of an ellipse and sets it equal to the perimeter of a circle with a radius of 2 ($2\pi^* r = p = 2\pi^*(a^2 + b^2)/2$).
[c]Equal to $100\ cm^3/a/b$.
[d]Equal to $2^*\pi^* r^*$length.
[e]Equal to surface area/$100\ cm^3$.

DOI: 10.1002/bdd

Table 5. Minimum and maximum A_I/V_a values for 100 and 1000 ml hemispherical *in vitro* dissolution vessels

Capacity	Diameter	Minimum aqueous volume[a]	Maximum aqueous volume[b]	Minimum A_I/V_a[c]	Maximum A_I/V_a[c]
ml	cm	ml	ml	cm^{-1}	cm^{-1}
100	4	27	50	0.25	0.47
1000 (USP II)	10	288	500	0.16	0.26

[a]Value gives minimum volume needed to achieve an aqueous liquid height high enough to allow for 1 cm below the bottom of the impeller for the 100 ml vessel (impeller is 0.8 cm tall) and 2.5 cm below the bottom of the 2 cm high impeller for the 1000 ml vessel (impeller is 2 cm tall) as well as 1 cm above the impeller for both vessels. Values calculated assuming a perfect hemispherical bottom.
[b]Value is half of the nominal capacity of the vessel, which assumes a 1:1 ratio of aqueous to organic medium.
[c]Minimum A_I/V_a is the aqueous-organic surface area divided by the maximum aqueous volume and maximum A_I/V_a is the aqueous-organic surface area divided by the minimum aqueous volume.

Rather than using geometrical considerations, Sugano used an equation relating human jejunal effective permeation rate to F_a to estimate A_I/V_a in humans *in vivo* to be about 2.3 cm^{-1} [31].[3] A_I/V_a was estimated in humans to be about $1.9 \pm 1.4\,cm^{-1}$ by dividing average k_a values from the literature for drugs dosed to humans that were passively absorbed, completely permeation rate limited, and at least 90% absorbed, by their estimated human jejunal permeation rate, which was estimated using molecular descriptors using model 1b from Winiwarter *et al*., 1998 [32]. Average A_I/V_a values in the range of 1.9 to 2.3 suggest percent compressions in the range of 60 to 70, which seem plausible anatomically. While it is convenient to assume an average human A_I/V_a, it is likely that this ratio varies based on differences in the volume of liquid and how it is distributed throughout the small intestine, and perhaps on the drug itself depending on the site of absorption.

Since the *in vitro* A_I/V_a is dictated by the diameter and geometry of the vessel, options for this parameter are limited if standard, hemispherical vessels are used. Table 5 shows the minimum and maximum A_I/V_a that can be achieved in a 1000 ml USP II vessel and a 100 ml vessel of similar proportions. These estimates are based on practical constraints such as maintaining a minimum aqueous volume to achieve a practical liquid height.

While P_I is dependent upon the properties of the drug substance and aqueous buffer, the diffusion layer thicknesses can be modified to some extent through the stirring rate, agitator length and design, and vessel geometry. A balance must be maintained between keeping the dosage form adequately suspended (if necessary), maintaining a level aqueous–organic interface with a well-defined surface area, and maintaining physiological hydrodynamics (if desired). Given these constraints, P_I is more of a defined rather than an adjustable parameter.

Given the somewhat limited range of *in vitro* A_I/V_a and the inability to fully control P_I, the desired k_p will not be achievable in all cases. Table 6 gives the estimated ranges for k_a and k_p for BCS II compounds. Since the range of k_p (0.002 to 50×10^4 cm/s) values envelops the range of estimated k_a values when A/V is assumed to be 2, there is a good chance that k_p may be obtained as desired in many cases. However, the ability to do so depends on the relationship between P_{eff} and P_I, which cannot be easily predicted.

In addition to maintaining the correct k_p and M_T/V_a values, ideally a two-phase experiment should be designed such that $F_{o,\infty}$ is similar to F_a *in vivo*. F_a can be estimated using Equation (25), where t_{res} is the residence time in the small intestine. An average value for t_{res} in the fasted human small intestine is about 3.5 h [5]. Once F_a has been estimated, the value of β required to achieve a $F_{o,\infty}$ similar to F_a can be determined using Equation (26). As K_{ap} increases, the required V_o relative to V_a needed to achieve a given $F_{o,\infty}$ decreases. An upper limit of a V_o that is three times V_a ($V_a/V_o \geq 0.33$) seems to be a practical cut-off for determining when the required V_o becomes impractical. When the Log K_{ap} of a compound at the desired pH is at least ~0.5 and V_a/V_o is at least 0.33, then $F_{o,\infty}$ is at least 0.90 ($\beta \leq$ ~0.11). The importance of K_{ap} can be demonstrated by examining the required *in vitro* V_a/V_o for metoprolol,

[3]In Sugano's analysis A_I/V_a is represented by A/V for a perfect cylinder times the Degree of Flatness (DF), such that A_I/V_a in our analysis = 2/r X DF in Sugano's analysis. They take r to be 1.5 cm in humans and DF to be 1.7.

DOI: 10.1002/bdd

Table 6. Estimated ranges of the average absorption rate coefficient *in vivo* (k_a) and the average partitioning rate coefficient *in vitro* (k_p) for BCS II compounds based on ranges for surface area to volume ratio *in vivo* (A/V) and *in vitro* (A_I/V_a), and average permeation rate *in vivo* (P_{eff}) and *in vitro* (P_I)

A/V[a]	$P_{eff} \times 10^4$[b]	$k_a \times 10^4$[c]	A_I/V_a[d]	$P_I \times 10^4$[e]	$k_p \times 10^4$[f]
cm^{-1}	cm/s	s^{-1}	cm^{-1}	cm/s	s^{-1}
2 *(1 to 7)*	1 to 14	2 to 28 *(1 to 100)*	0.16 to 0.47	0.01 to 100	0.002 to 50

[a]Estimated based on an A/V of 2 and plausible percent compression based on Table 2.
[b]Approximate range for measured human jejunal effective permeation rate for BCS II compounds from reference [32].
[c]Calculated – equal to $A/V * P_{eff} \times 10^4$.
[d]Range from Table 1 assuming standard USP guidelines for impeller positioning.
[e]Estimated using equation 28 assuming h_a from 10 to 50 μm and D_a from 10^{-5} to 10^{-7} cm^2/s.
[f]Calculated – equal to $A_I/V_a * P_I \times 10^4$.

which is used as a reference compound to designate drug substances as having low or high permeability according to the BCS [33]. Greater than 90% of an oral dose of metoprolol is known to be absorbed in the small intestine. Metoprolol has a log P of 2.2 (neutral species), but a log K_{ap} of about −0.8 at pH 6.5 [34], which is often taken to be the average fasted state pH in the upper small intestine. Because of its low K_{ap} in the intestinal pH range, 6 litres of 1-octanol would be required to achieve a $F_{o,\infty}$ of 0.9 (V_a/V_o of 1/60), making metoprolol a less than ideal candidate for the two-phase system despite its high extent of *in vivo* absorption. However, for ibuprofen, which is > 99% absorbed in humans and has a calculated Log K_{ap} of 1.7 at pH 6.5, only 200 ml of 1-octanol would be needed to achieve a $F_{o,\infty}$ of 0.99 (V_a/V_o of 1/2) [35].

$$F_a = 1 - e^{-k_a t_{res}} \tag{25}$$

$$\beta = \frac{V_a}{K_{ap} V_o} = \frac{1 - F_a}{F_a} \tag{26}$$

We present a few case studies to demonstrate how a two-phase system would be set up to mimic *in vivo* absorption rate for a few compounds for which *in vivo* k_a values have already been determined in humans. We took the k_a values of four compounds dosed as oral solutions (ibuprofen, valproic acid, felodipine and ondansetron) from the publication by Linnankoski *et al.* [36] that were passively absorbed, demonstrated completely permeation rate-limited absorption, had F_a values of one, and had calculated Log D values at pH 6.5 (average fasted human intestinal pH [5]) greater than one. We then used our proposed scaling factors, A_I/V_a, M_T/V_a and $V_a/(K_{ap}\ V_o)$ to estimate the vessel size, aqueous volume, organic volume and dose that would be required to achieve a 'physiological two-phase set-up' for these compounds when performing two-phase dissolution experiments, as outlined below.

1. Determine dissolution vessel size and *in vitro* V_a using A_I/V_a.

- Estimate k_a *in vivo*.
- Estimate P_I using Equation (10) with the following values.
  - Estimate D_a using Hayduk-Laudie method.
  - Assume h_a equals 30 μm.
  - $K_{ap} = 10^{\text{cLogD } 6.5}$
- Estimate desired A_I/V_a using Equation (24).
- Determine which dissolution vessel size can achieve similar A_I/V_a (with the preference being a 1000 ml USP 2 vessel using the standard set-up for stirrer position) and which value of V_a must be used to achieve that value.

2. Determine M_T (dose *in vitro*) using M_T/V_a.

- Estimate *in vivo* dose/V (dose/100 ml in fasted humans).
- M_T *in vitro* = (*in vivo* dose/V) * V_a

3. Determine V_o *in vitro* using $\beta = V_a/(K_{ap}\ V_o)$.

- Determine F_a *in vivo* using Equation (25).
- Determine ideal β *in vitro* using Equation (26).
- $V_o = V_a/(10^{\text{cLogD } 6.5} * \beta)$. Select V_o such that $F_{o,\infty}$ is within 10% of F_a.

The results are tabulated in Table 7. Valproic acid requires a high A_I/V_a of 0.52, which is at

DOI: 10.1002/bdd

Table 7. Desired and achievable *in vitro* two-phase parameters to make dissolution test physiological for valproic acid, ondansetron, ibuprofen and felodipine based on *in vivo* properties and performance

	In vivo properties/ performance					*In vitro* drug properties			Desired *in vitro* parameters				Achievable *in vitro* parameters							
	F_a[a]	k_a[a] $\times 10^4$	Dose[b]	V[c]	Dose $/V$	clog$D$ 6.5[d]	D_a[e] $\times 10^6$	P_I[f] $\times 10^4$	k_p[g] $\times 10^4$	A_I/V_a[h]	F_{o_∞}[i]	M_T/V_a[j]	Vessel capacity	Depth below impeller[k]	Vessel A_I/V_a[l]	V_a[m]	k_p[n] $\times 10^4$	V_o[o]	β	Dose[p]
	Actual	Decon.	Theo.	Est.	Est.	Calc.	Est.	Est.	Based on k_a	Est.		Based on dose/V		Based on USP standard		Req.	Est.	Req.		Req.
Drug name		s^{-1}	mg	ml	mg/ml	-	cm^2/s	cm/s	s^{-1}	cm^{-1}	-	mg/ml	ml	cm	cm^{-1}	ml	s^{-1}	ml	-	mg
Valproic acid (BCS II)	1	11.5	250	100	2.50	1.43	8.87	22.1	11.5	0.52	0.98	2.50	100	1.0	0.47	27	10.4	50	0.02	68
Ondansetron (BCS I or III)	1	5.3	8	100	0.08	1.65	6.63	18.4	5.3	0.29	0.98	0.08	1000 (USP II)	2.5	0.26	302	4.8	338	0.02	24
Ibuprofen (BCS II)	1	7.4	200	100	2.00	2.19	7.50	23.6	7.4	0.31	0.98	2.00	1000 (USP II)	2.5	0.26	302	6.1	97	0.02	604
Felodipine (BCS II)	1	12.5	5	100	0.05	3.41	6.10	20.3	12.5	0.62	0.98	0.05	Not possible unless depth below impeller is decreased to 2 cm and smaller vessel used							

[a]From reference [36].
[b]Arbitrarily chose one of the marketed oral unit doses.
[c]Average human fasted intestinal volume.
[d]Determined using reference [26].
[e]Estimated using Hayduk-Laudie (H-L) method.
[f]Estimated using Equation (10) assuming $h_a = h_o = 30\ \mu m$.
[g]Equal to k_a.
[h]Calculated using Equation (24).
[i]Value should ideally be equal or close to Fa *in vivo*. 0.98 was chosen due to vessel size constraints.
[j]Equal to Dose/V.
[k]The standard set-up for distance from bottom of vessel to bottom of impeller is 2.5 cm for the 1000 ml USP 2 vessel. 1 cm chosen for 100 ml vessel, which should accommodate a tablet or capsule.
[l]From Table 1. Value set by apparatus geometry and minimum or maximum practical volume of media.
[m]Volume required to achieve A_I/V_a.
[n]Equal to estimated P_I times the actual A_I/V_a.
[o]Volume required to achieve desired $F_{o,\infty}$ based on *c*Log*D* 6.5 and V_a.
[p]Equal to desirable M_T/V_a * achievable V_a.

DOI: 10.1002/bdd

the top of the achievable range. An A_I/V_a as high as about 0.47 can be achieved with a standard 100 ml vessel and minimum height of 1 cm below the impeller. Ibuprofen and ondansetron require A_I/V_a values of 0.29 and 0.31, respectively. Values in this range can be achieved with any vessel in the range of 100 to 1000 ml. Felodipine requires an A_I/V_a of 0.62, which cannot be achieved conveniently in the two-phase system. Figure 7 compares the average *in vivo* absorption profiles using the given k_a values with the predicted *in vitro* partitioning profiles using the k_p values from Table 7 for ibuprofen, valproic acid and ondansetron. Despite the differences between k_a and k_p due to the constraints of the vessels, the *in vitro* and *in vivo* curves match up quite well, demonstrating similarities between *in vivo* absorption and predicted *in vitro* two-phase partitioning profiles of drugs in solution that result when the apparatus is scaled using the parameters A_I/V_a, M_T/V_a and $V_a/(K_{ap}\ V_o)$.

The purpose of these case studies is to demonstrate how a two-phase system can be set-up to be physiologically relevant when conducting an experiment using a solid dosage form. When these scaling parameters are maintained at physiological values as described above, and a physiological aqueous buffer is used, the saturation conditions in the aqueous medium of the two-phase system are expected to be similar to saturation conditions *in vivo*, and the *in vitro* partitioning rate is expected to be similar to the *in vivo* absorption rate, facilitating potential IVIVCs for some drug candidates as described in the next section.

Potential drug candidates

Two-phase dissolution apparatuses can be useful tools to scientists developing solid oral drug formulations. As no one dissolution apparatus currently captures the range of physiological conditions affecting dissolution and absorption, it is important that the chosen apparatus encompasses the most important factors for the particular drug product of interest. If the key physiological scaling parameters (A_I/V_a, M_T/V_a and $V_a/(K_{ap}\ V_o)$) for the two-phase system described above are properly designed, and a physiological aqueous buffer is used, it is reasonable to expect similar saturation conditions between the *in vitro* aqueous medium and the intestinal lumen and to expect an *in vitro* partitioning rate that is similar to the *in vivo* absorption rate of a drug substance. However, an IVIVC has the potential to be developed only for drug substances for which the F_a is similar to the fraction bioavailable. Thus, for a drug substance to be a candidate for the two-phase system it should have

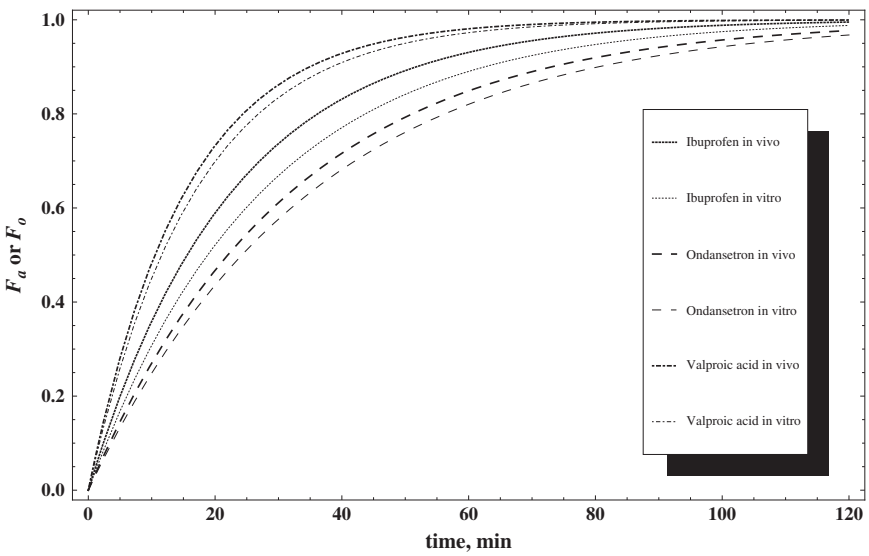

Figure 7. Comparison of fraction absorbed *in vivo* (in humans) and estimated fraction partitioned in 1-octanol *in vitro* in a 1000 ml USP 2 vessel for ibuprofen and ondansetron, and a 100 ml hemispherical vessel for valproic acid using the simplified model

DOI: 10.1002/bdd

a relatively high F_a *in vivo*, should be relatively hydrophobic (i.e. Log K_{ap} at pH 6.5 should be greater than about ~0.5–1 so a practical volume of organic medium can be used to achieve an extent of *in vitro* partitioning that is similar to the F_a), and its F_a should be similar to its fraction bioavailable (i.e. low first-pass metabolism and gut metabolism/degradation).

The feasibility of using the two-phase system to predict *in vivo* performance should be verified by properly scaling the apparatus as discussed above and performing experiments using solid dosage forms of drugs with different physicochemical properties (e.g. acid-base character, particle size, pH-solubility profile, human jejunal effective permeation rate, dose), using relevant aqueous media types (e.g. surfactant level, buffer species, constant or variable pH). In each case, solubility and dissolution rate of drug in the chosen buffer should be compared with solubility and dissolution rate of drug in the chosen buffer saturated with organic medium. Unpublished data from our laboratory shows no difference between dissolution rates of ibuprofen particles in sodium acetate buffer (50 mM, pH 4.5, isotonic) and sodium acetate buffer saturated with 1-octanol. However, the presence of organic medium in buffer containing surfactant could have greater effects on solubility and dissolution rate as well as on rate and extent of partitioning into the organic medium [37]. Research has shown that long-chain alcohols such as 1-octanol can form mixed micelles with ionic surfactants [38]. Depending on the relative concentrations of the long-chain alcohol and surfactant, the alcohol can decrease the critical micelle concentration (CMC) of surfactant, increase the ionization of micelles, and change the micellar size and structure [38,39].

In addition to the possible impact of surfactants on dosage form performance in the two-phase apparatus, integrity of the aqueous–organic interface should also be considered. Shi *et al*. successfully performed two-phase experiments at polysorbate 80 concentrations as high as 0.23 mM [11]. We have demonstrated the formation of a clear, distinct aqueous-organic interface using Fasted State Simulated Intestinal Fluid and Fed State Simulated Intestinal Fluid (Phares FaSSIF and FeSSIF, Muttenz, Switzerland), and 0.7 mM sodium dodecyl sulphate (SDS) in a USP II apparatus as 25, 50 and 75 rpm (unpublished data). The interface was somewhat obscured at 100 rpm. However, we recommend running USP II two-phase experiments at speeds lower than 75 rpm to minimize formation of a vortex.

Since the two-phase system adds a level of complexity compared with single-phase systems it is also important to outline for which drug substances and drug products a two-phase system may lead to improved IVIVCs over a single-phase system that employs a large aqueous volume (e.g. 900 ml). A two-phase system will likely be more useful when dissolution is limited by solubility (i.e. dose number is high), which often occurs when solubility is low and dose is moderate-to-high. In this situation the drug saturation profile in the aqueous medium will likely be different in a two-phase system with 100 ml of aqueous buffer and a sufficient volume of organic medium to achieve physiologically relevant extent and rate of partitioning than it would be in a single-phase system with 900 ml of medium. Another case when a two-phase system may provide an improved IVIVC over a single-phase system is when the rate of appearance of drug in the organic medium is limited at least in part by permeation rate, which can occur for drugs with low to moderate average intestinal permeation rates.

In general, a two-phase test may be most useful for some BCS II compounds (which often have solubility limitations), but may presumably also be useful for some BCS IV compounds (which often have solubility and permeation rate limitations). As each class contains drugs with a range of properties, it will be important to assess the potential applicability of two-phase systems based on key drug physicochemical properties such as acid-base character, particle size, pH-solubility profile, human jejunal effective permeation rate and dose.

Conclusion

Two-phase dissolution apparatuses simultaneously capture the processes of drug dissolution and partitioning, thereby simulating absorption while maintaining a physiological volume of buffer. They have the potential to provide meaningful predictions of *in vivo* performance for some

DOI: 10.1002/bdd

drug products, and can therefore be useful tools to industrial and academic scientists for designing and developing drug product formulations.

While researchers have been exploring the utility of two-phase systems for simple and novel oral dosage forms since the 1960s, and have shown improved predictive capabilities over conventional methods, no one has elucidated the mechanism by which two-phase dissolution apparatuses may facilitate improved IVIVCs over conventional single-phase systems, or determined for which drugs and dosage forms these apparatuses could be most useful. We performed a mechanistic, drug-transport analysis of the partitioning of solutes in solution in an *in vitro* two-phase dissolution apparatus, and demonstrated the ability of our model to successfully describe the *in vitro* partitioning profiles of three BCS II weak acids in four different experimental set-ups. In contrast to previous kinetically derived mathematical models, our model uses physical input parameters that are known or can be estimated *a priori*. To establish the physiological relevance of the test for the drug product of interest, we have proposed scaling factors (A_I/V_a, M_T/V_a and $V_a/(K_{ap}\ V_o)$), the values of which can be determined based on molecular descriptors. When these scaling parameters are maintained at physiologically relevant values and a physiological aqueous buffer is used, the saturation conditions in the aqueous medium of the two-phase system are expected to be similar to saturation conditions *in vivo*, and the *in vitro* partitioning rate is expected to be similar to the *in vivo* absorption rate. Potential IVIVCs between the *in vitro* partitioning and *in vivo* absorption profiles may result for some drug products that have relatively high fraction absorbed values and low extents of hepatic first-pass metabolism and gut degradation/metabolism. While this manuscript focuses on an analysis of drugs in solution, these scaling factors can be applied to dissolution of solid dosage forms in two-phase dissolution apparatuses, which will be the focus of future work.

The two-phase system may be a more physiologically relevant tool than a conventional single-phase system for some BCS II, and possibly some BCS IV drugs. Although the dissolution-partitioning behaviour of a drug dosage form is complex and dependent upon drug physicochemical properties, dose, permeation rate, dosage form type and formulation composition, it is probable that two-phase systems may be particularly useful for drug products that experience solubility-limited dissolution and/or a permeation rate limitation *in vivo*, or include functional excipients that may affect dissolution and/or absorption at physiological concentrations. To help determine the general applicability of the two-phase system and provide recommendations for determining for which drugs and dosage forms a two-phase dissolution apparatus may be most useful, our mass transport analysis could be extended to include simultaneous dissolution and partitioning of drug substances from dosage forms, and tested in a two-phase system using solid dosage forms of drugs with different physicochemical properties (such as acid-base character, particle size, pH-solubility profile, human jejunal effective permeation rate, and dose) using relevant aqueous media types. The *in vivo* relevance could be ascertained by performing studies in dogs or humans (or by using existing *in vivo* data from the literature) and comparing the deconvoluted *in vivo* absorption profiles with the *in vitro* organic phase partitioning profiles.

Acknowledgements

We would like to thank Yeo Jung Park for performing the non-linear regression analysis of the *in vitro* partitioning data, and Kerby Shedden PhD for his assistance in designing the analysis. We would also like to thank Nicholas Waltz for his work in conducting some of the partitioning experiments.

We gratefully acknowledge funding support from Abbott Laboratories, North Chicago, IL, the American Foundation for Pharmaceutical Education (AFPE), and the National Institute of General Medical Sciences (NIGMS) grant number GM007767.

The contents of this manuscript are solely the responsibility of the authors and do not necessarily represent the official views of NIGMS.

Conflict of Interest

The authors declare that there is no conflict of interest.

DOI: 10.1002/bdd

References

1. Abdou HM. *Effect of the physicochemical properties of the drug on dissolution rate. Dissolution, Bioavailability and Bioequivalence*. Mack Publishing: Easton, PA, 1989; 56–72.
2. Sheng J. *Toward an In Vitro Bioequivalence Test*. University of Michigan: Ann Arbor, 2007.
3. Amidon GL, Lennernas H, Shah VP, Crison JR. A theoretical basis for a biopharmaceutic drug classification: The correlation of *in vitro* drug product dissolution and *in vivo* bioavailability. *Pharm Res* 1995; **12**: 413–420. DOI: 10.1023/A:1016212804288.
4. FDA. *Guidance for Industry. Waiver of the In Vivo Bioavailability and Bioequivalence Studies for Immediate-Release Solid Oral Dosage Forms Based on a Biopharmaceutics Classification System*. U.S. Department of Health and Human, Food and Drug Administration (FDA), Center for Drug Evaluation and Research: Washington, DC, 2000.
5. Mudie DM, Amidon GL, Amidon GE. Physiological parameters for oral delivery and *in vitro* testing. *Mol Pharm* 2010; **7**: 1388–1405. DOI: 10.1021/Mp100149j.
6. Pillay V, Fassihi R. A new method for dissolution studies of lipid-filled capsules employing nifedipine as a model drug. *Pharm Res* 1999; **16**: 333–337. DOI: 10.1023/A:1011959914706.
7. Hoa NT, Kinget R. Design and evaluation of two-phase partition-dissolution method and its use in evaluating artemisinin tablets. *J Pharm Sci* 1996; **85**: 1060–1063. DOI: 10.1021/js960115u.
8. Gabriels M, Plaizier-Vercammen J. Design of a dissolution system for the evaluation of the release rate characteristics of artemether and dihydroartemisinin from tablets. *Int J Pharm* 2004; **274**: 245–260. DOI: 10.1016/j.ijpharm.2004.01.022.
9. Grundy JS, Anderson KE, Rogers JA, Foster RT. Studies on dissolution testing of the nifedipine gastrointestinal therapeutic system. 2. Improved *in vitro in vivo* correlation using a two-phase dissolution test. *J Control Release* 1997; **48**: 9–17. DOI: 10.1016/S0168-3659(97)01638-6.
10. Heigoldt U, Sommer F, Daniels R, Wagner KG. Predicting *in vivo* absorption behavior of oral modified release dosage forms containing pH-dependent poorly soluble drugs using a novel pH-adjusted biphasic *in vitro* dissolution test. *Eur J Pharm Biopharm* 2010; **76**: 105–111. DOI: 10.1016/J.Ejpb.2010.05.006.
11. Shi Y, Gao P, Gong YC, Ping HL. Application of a biphasic test for characterization of *in vitro* drug release of immediate release formulations of celecoxib and its relevance to *in vivo* absorption. *Mol Pharm* 2010; **7**: 1458–1465. DOI: 10.1021/Mp100114a.
12. Grassi M, Coceani N, Magarotto L. Modelling partitioning of sparingly soluble drugs in a two-phase liquid system. *Int J Pharm* 2007; **239**: 157–169. DOI: 10.1016/S0378-5173(02)00101-1.
13. Takayama K, Nambu N, Nagai T. Analysis of interfacial transfer of indomethacin following dissolution of indomethacin-polyvinylpyrrolidone coprecipitates. *Chem Pharm Bull* 1981; **29**: 2718–2721.
14. Suzuki A, Higuchi WI, Ho NFH. Theoretical model studies of drug absorption and transport in gastrointestinal tract. 1. *J Pharm Sci* 1970; **59**: 644–651. DOI: 10.1002/jps.2600590514.
15. Ingram T, Richter U, Mehling T, Smirnova I. Modelling of pH dependent n-octanol/water partition coefficients of ionizable pharmaceuticals. *Fluid Phase Equilibr* 2011; **305**: 197–203. DOI: 10.1016/J.Fluid.2011.04.006.
16. Hayduk W, Laudie H. Prediction of diffusion-coefficients for nonelectrolytes in dilute aqueous-solutions. *Aiche J* 1974; **20**: 611–615. DOI: 10.1002/aic.690200329.
17. Othmer DF, Thakar MS. Correlating diffusion coefficients in liquids. *Ind Eng Chem* 1953; **45**: 589–593. DOI: 10.1021/ie50519a036.
18. Korson L, Drosthan W, Millero FJ. Viscosity of water at various temperatures. *J Phys Chem* 1969; **73**: 34–39. DOI: 10.1021/j100721a006.
19. Seki T, Mochida J, Okamoto M, *et al*. Measurement of diffusion coefficients of parabens and steroids in water and 1-octanol. *Chem Pharm Bull* 2003; **51**: 734–736.
20. Vandewaterbeemd JTM, Vanboekel CCA, Desevaux RLF, *et al*. Transport in Qsar-IV – the interfacial drug transfer model – relationships between partition-coefficients and rate constants of drug partitioning. *Pharm Weekblad* 1981; **3**: 224–225.
21. Yalkowsky SH, Valvani SC, Roseman TJ. Solubility and partitioning. 6. Octanol solubility and octanol–water partition-coefficients. *J Pharm Sci* 1983; **72**: 866–870.
22. Pinsuwan S, Li A, Yalkowsky SH. Correlation of octanol water solubility ratios and partition-coefficients. *J Chem Eng Data* 1995; **40**: 623–626. DOI: 10.1021/je00019a019.
23. Sangster J. *Octanol–Water Partition Coefficients: Fundamentals and Physical Chemistry*. John Wiley & Sons: Chichester, 1997.
24. Mannhold R, Poda GI, Ostermann C, Tetko IV. Calculation of molecular lipophilicity: state-of-the-art and comparison of Log P methods on more than 96,000 compounds. *J Pharm Sci* 2009; **98**: 861–893. DOI: 10.1002/Jps.21494.
25. Hidalgo IJ, Hillgren KM, Grass GM, Borchardt RT. Characterization of the unstirred water layer in Caco-2 cell monolayers using a novel diffusion apparatus. *Pharm Res* 1991; **8**: 222–227. DOI: 10.1023/A:1015848205447.
26. ChemAxon L. MarvinSketch 5.6.0.1. MarvinSketch 5.6.0.1 ed. 2011.
27. Yazdanian M, Glynn SL, Wright JL, Hawi A. Correlating partitioning and Caco-2 cell permeability of structurally diverse small molecular weight compounds. *Pharm Res* 1998; **15**: 1490–1494. DOI: 10.1023/A:1011930411574.

28. Schiller C, Frohlich C, Giessmann T, *et al*. Intestinal fluid volumes and transit of dosage forms as assessed by magnetic resonance imaging. *Aliment Pharmacol Ther* 2005; **22**: 971–979. DOI: 10.1111/j.1365-2036.2005.02683.x.
29. Linnankoski J, Ranta VP, Yliperttula M, Urtti A. Passive oral drug absorption can be predicted more reliably by experimental than computational models – fact or myth. *Eur J Pharm Sci* 2008; **34**: 129–139. DOI: 10.1016/J.Ejps.2008.03.001.
30. Simulations Plus Admet Predictor version 5.5. 2011.
31. Sugano K. Theoretical investigation of passive intestinal membrane permeability using Monte Carlo method to generate drug-like molecule population. *Int J Pharm* 2009; **373**: 55–61. DOI: 10.1016/J.Ijpharm.2009.02.002.
32. Winiwarter S, Ax F, Lennernas H, *et al*. Hydrogen bonding descriptors in the prediction of human *in vivo* intestinal permeability. *J Mol Graph Model* 2003; **21**: 273–287. DOI: 10.1016/S1093-3263(02)00163-8.
33. Takagi T, Ramachandran C, Bermejo M, *et al*. A provisional biopharmaceutical classification of the top 200 oral drug products in the United States, Great Britain, Spain, and Japan. *Mol Pharm* 2006; **3**: 631–643. DOI: 10.1021/Mp0600182.
34. Dahan A, Miller JM, Hilfinger JM, *et al*. High-permeability criterion for BCS Classification: Segmental/pH dependent permeability considerations. *Mol Pharm* 2010; **7**: 1827–1834. DOI: 10.1021/Mp100175a.
35. Potthast H, Dressman JB, Junginger HE, *et al*. Biowaiver monographs for immediate release solid oral dosage forms: Ibuprofen. *J Pharm Sci* 2005; **94**: 2121–2131. DOI: 10.1002/Jps.20444.
36. Linnankoski J, Makela JM, Ranta VP, *et al*. Computational prediction of oral drug absorption based on absorption rate constants in humans. *J Med Chem* 2006; **49**: 3674–3681. DOI: 10.1021/Jm051231p.
37. Sugano K. Computational oral absorption simulation for low-solubility compounds. *Chem Biodivers* 2009; **6**: 2014–2029.
38. Moya SE, Schulz PC. The aggregation of the sodium dodecyl sulfate *n*-octanol water system at low concentration. *Colloid Polym Sci* 1999; **277**: 735–742.
39. Dubey N. Micellar properties and related thermodynamic parameters of aqueous anionic surfactants in the presence of monohydric alcohols. *J Chem Eng Data* 2011; **56**: 3291–3300. DOI: 10.1021/Je101358p.
40. Levis KA, Lane ME, Corrigan OI. Effect of buffer media composition on the solubility and effective permeability coefficient of ibuprofen. *Int J Pharm* 2003; **253**: 49–59. DOI: 10.1016/S0378-5173(02)00645-2.
41. Avdeef A, Voloboy D, Foreman A. *Dissolution and Solubility*. Elsevier: Amsterdam, 2007.